Influence of the Radicaloid Character of Polyaromatic Hydrocarbon Couplers on Magnetic Exchange Interactions

Prabhleen Kaur and Md.Ehesan Ali*

Institute of Nano Science and Technology, Sector-81, Mohali, Punjab 140306, India

E-mail: ehesan.ali@inst.ac.in

Abstract

Understanding the properties of the coupler influencing spin-spin interactions in organic diradicals are crucial for designing of molecular spintronic systems with long-range effects. In this quest, using density functional theory (DFT) based broken symmetry method, magnetic exchange coupling ($2J$) between localized radical centers at a given length connected via spacers with different radicaloid character (y) is investigated. The nitroxy radical sites are coupled through prototypical decacene coupler keeping them ~ 27 $\AA$ apart. Couplers with different y values, modeled by addition of benzenoid rings in the spin confining region of decacene are used as different spacers between nitroxide diradicals. The strength of magnetic coupling between the localized spin centers is found to be correlated with the radicaloid character of polyaromatic hydrocarbon (PAH) spacers. The stronger exchange interaction is observed for the diradical with higher radicaloid character. It is further observed that the fractional occupied molecular orbitals (MOs) responsible for the open-shell nature of the coupler predominantly constitute the Frontier MOs (FMOs), while in diradicals SOMOs constitute the FMOs.

Introduction

Organic radicals have gained an enormous attention in the recent years due to their potential applications in the field of molecular electronics,[1] spintronics,[2] non-linear optics, organic field effect transistors (OFETs),[3] quantum computers[4,5] and two-photon absorption (TPA),[6] etc. One of the peculiar property that separates zigzag edges in nanometer graphytic systems from armchair edges is the localization of spins at these zigzag edges.[7–10] Among these are, fragments of graphene like triangulene which have drawn a lot of attention to having potential applications in the field of spintronics, bringing within the reach an access to high-spin ground states in carbon-based materials.[11–14] Despite the experimental challenges arising due to open-shell nature in zigzag edged based nanographene structures, studies have branched into designing devices combining the topological effects of zigzag edge extensions to induce local magnetic moments.[15,16]

Recently, surge has been found in studying radicaloid properties of these carbon based molecules and their influence on other physical properties.[17,18] Rudebusch et al. have synthesised an air- and temperature stable diindeno[b,i]anthracene (DIAn) molecule with a potential application in the field of OFETs owing to it's radicaloid nature.[19] Koike et al. showed highly crystalline Ph_2-IDPL have high mobility because of strong intermolecular interactions aided by open-shell singlet (OSS) nature of these molecules.[20] Ni et al. reported that para- and meta-quinodimethane BODIPY dimers having low to moderate radicaloid character could be potential candidates for NIR dyes.[21] Yang and co-workers have experimentally showed an increased electrical conductivity and thermoelectric properties of organic molecules owing to their radicaloid characters.[22,23] Ullrich et al. synthesised carbene derived singlet fission molecules by dimer assembly and having high radicaloid characater in dimeric form.[24]

Correlations between aromaticity and radicaloid character has been theoretically investigated independently by Ito et al.[25] and Pinheiro et al.[26] deducing an inverse relationship between the afore mentioned chemical properties. Research has also advanced in tuning the radicaloid

properties of the molecules by doping, plane twisting and changing aromaticity. Theoretical studies on tuning the radical character by attaching aromatic ring in the base structure and by π-plane twisting has been suggested as an improvement over potential singlet fission organic molecule candidates by Ito et al.[27] A study on tuning the radicaloid character of higher acenes with symmetric doping of two C atoms with two Nitrogen or two Boron atoms was done by Pinheiro et al. showing that doping into outer rings leads to an increase in radical character whereas doping central β C's leads to decrease in radical character as compared to pristine acene.[28] Pinheiro and co-workers theoretically studied the effects of Boron and Nitrogen doping in tetracene to fine tune radicaloid properties along with chemical stability to design prudent candidates for singlet fission sensitizers.[29] A topological modification of acenes by introducing cyclobutadiene linkage in the center as studied by Milanez et al. drastically affects the aromaticity of the directly fused benzene rings, reduces overall radicaloid nature and increases chemical stability as compared to pristine acenes.[30]

Magnetic exchange coupling ($2J$) between organic radicals *via* non-magnetic spacers has been widely studied.[31–34] Various factors controlling the magnetic exchange like torsional angle between the radical sites and the coupler, length of the coupler[35,36] and the π-conjugations of the coupler have been explored and found to have a crucial role in deciding the nature and magnitude of magnetic exchange coupling. The magnetic exchange coupling constants have been observed to decay exponentially with the increase in the coupler length.[37,38] Among several spacers, π-conjugated spacers are best suited to have long-range magnetic exchange interactions.[39,40] However, the influence of the radical nature of the spacer itself on mediating the magnetic exchange interactions has not been addressed in the literature in details.[41,42] Understanding the correlation between magnetic coupling and radicaloid nature of the spacer will provide an additional window to modulate the intramolecular magnetic exchange interactions.[43,44]

In the present work, we aim to find the relation between the magnetic exchange coupling constants ($2J$) of localized spins and the radicaloid character (y) of the an open-shell sin-

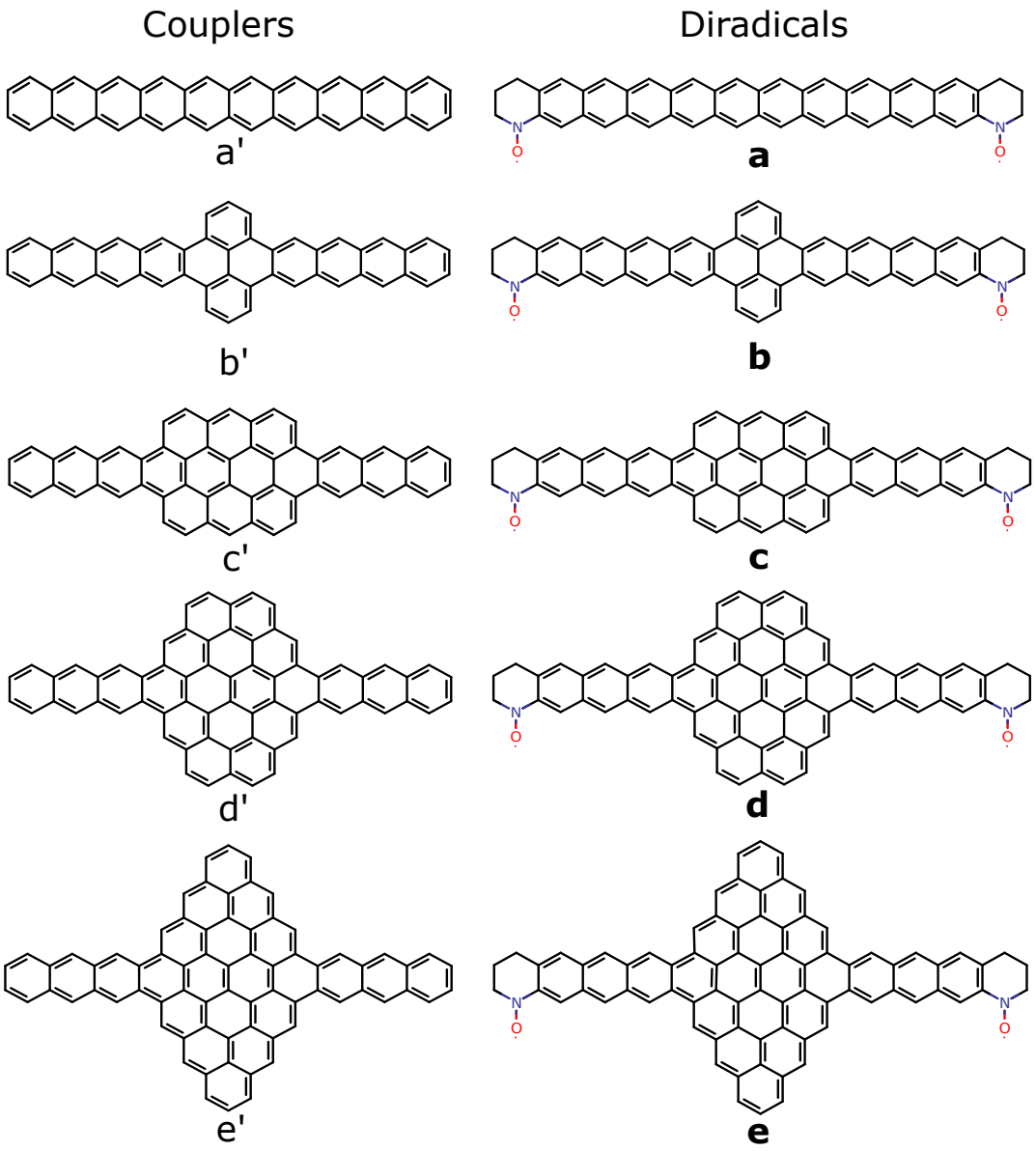

Figure 1: The spacers used in this study are shown on the left side in the figure (a′ - e′). Decacene (a′) is chosen as the prototypical coupler. Other couplers are modeled by adding benzenoid rings on both the zigzag edges of decacene starting from high spin-density central region (b′ - e′). Magnetic exchange coupling constants were found for meta- connected nitroxy diradicals through these spacers (**a** - **e**), represented on the right side in the figure. These diradicals are modeled such that the distance between the nitroxy radical sites is constant of ~ 27 $\mathring{A}$ while the conjugation in the coupler changes profoundly.

glet (OSS) coupler mediating this magnetic exchange. To do so, decacene is chosen as the prototypical coupler having high radicaloid character owing to its OSS nature and promoting long-range interactions as explicitly investigated in our previous study.[44] The couplers (Figure 1 (b′ - e′)) are then modeled from this base decacene spacer by step-wise addition of benzenoid rings protruding from decacene's central benzene rings. This leads to increase in the π-conjugation having zigzag edge topologies extending from center starting from cove-type edge[45] (b′) to [3]triangulene (e′) type nanostructures on either side of decacene zigzag edge. These couplers are used to mediate between meta- connected nitroxide diradicals (Figure 1 (**a** - **e**)) and then the magnetic exchange coupling between these nitroxy radicals are computed. Such diradicals have fixed distance of ~ 27 $\mathring{A}$ between nitroxide radical sites but with couplers having different radicaloid character (y).

Computational Details

All the organic spacers and diradicals under study (Figure 1) were optimized within the density functional theory (DFT) regime. Becke's three-parameter and Lee-Yang-Parr's exchange-correlation hybrid functional (B3LYP)[46] with atom centered polarized triple-zeta (def2-TZVP)[47,48] basis sets in triplet/OSS states are employed in quantum chemistry code ORCA.[49] To speed up the calculations, resolution of identity (RI) approximation along with auxiliary basis set def2/J has been used with chain of spheres (COSX) numerical integration[50] with a convergence criteria of 10^{-8} Eh for each electronic step. Triplet spin state was found to be the ground state for all the modeled diradicals (**a** - **e**) therefore, these geometries were used for computing magnetic properties of these molecular systems. While couplers (a′ - e′) have OSS as their ground state therefore, OSS geometries have been used to compute coupler properties.

The magnetic exchange coupling between the two magnetic centers 'a' and 'b' is expressed

by the Heisenberg-Dirac-van Vleck (HDvV) spin Hamiltonian:

$$\hat{H}_{HDvV} = -2J\hat{S}_a.\hat{S}_b \tag{1}$$

where $2J$ is the orbital-averaged effective exchange integral between the spin sites a and b, $\hat{S}_a$ and $\hat{S}_b$ being the respective spin operators of these sites. The positive sign of $2J$ indicates ferromagnetic and the negative sign indicates antiferromagnetic interactions. In this work, the magnetic coupling constants have been evaluated by employing the broken symmetry unrestricted density functional theory (BS-DFT) approach with the formalism proposed by Noodleman and coworkers.[51] In this formalism, after obtaining the spin-unrestricted solutions for the determinant of maximum spin $M_S = |S_a + S_b|$ and the broken spin symmetry $M_S = |S_a - S_b|$, the formula for coupling constant is expressed as:

$$2J = 2\Big(\frac{E_{BS} - E_{HS}}{\hat{S}^2_{max}}\Big) \tag{2}$$

where E_{BS} and E_{HS} represent the energies of broken symmetry and high spin states respectively. The BS solution obtained is not an eigenfunction of the Hamiltonian, but is an admixture of the singlet and triplet states. The overlap integral between magnetic orbital was neglected in this formalism. In principle, the singlet-state requires a multi-determinant representation of wave function which cannot be obtained accurately in a single-determinant approach. However, standard broken symmetry DFT is found to be a successful method in extracting the magnetic coupling constants ($2J$) for the organic diradicals.[52,53]

Calculation of radicaloid character of the coupler (y)

The radicaloid character of the coupler has been calculated from the occupancy of unrestricted Hartree-Fock (UHF) based molecular orbitals as proposed by Yamaguchi et al.[54,55]

given in terms of diradical character (y) by:

$$y = 1 - \frac{2T}{1+T^2} \tag{3}$$

where

$$T = \frac{n_{HONO} - n_{LUNO}}{2} \tag{4}$$

where n_{HONO} and n_{LUNO} are the occupancies of the frontier natural orbitals. Radicaloid character (y) has been calculated from the ground state natural orbital occupancy of the molecular system. The natural orbital occupancy of the frontier orbitals from OSS state of the couplers (a′ - e′) is used to evaluate their radicaloid character. Whereas, natural orbital occupancy from the triplet state has been used for couplers in diradicals (**a-e**). To evaluate y for couplers in **a-e**, n_{HONO} and n_{LUNO} were the natural orbital occupations of the orbitals just before the SOMOs and just after the SOMOs respectively. The evaluation of y from SOMO's would simply give y=1, describing a diradical system. Presence of two nitroxy radicals already adheres to diradical, therefore to evaluate radical property of the coupler in **a-e**, natural occupancy of frontier orbitals after excluding SOMOs is used.

Results and discussion

The higher-order polyaromatic hydrocarbons (PAHs) are found to have an open-shell singlet (OSS) electronic structure as their ground state. The extent of open-shell nature of such systems is quantified in terms of their radicaloid character (y) which is computed from the natural orbital occupation number of the frontier orbitals.[54,55] The value of y can range from 0 to 1, where $y = 1$ indicates purely open-shell molecule and $y = 0$ corresponds to closed shell molecular system. Computed y_p values of studied PAH couplers (a′ - e′) along with their singlet-triplet energy gaps are tabulated in Table 1. It has been already established that there is an inverse relation between ΔE_{S-T} and y.[56] From Table 1 also it is observed that

Table 1: Singlet-triplet (ΔE_{S-T}) (kcal/mol) gap for PAH couplers computed with B3LYP/def2-TZVP method and their radicaloid characters (y_p) calculated from natural orbital occupancy of frontier orbitals obtained with UHF/def2-TZVP method.

PAH coupler	E_{HS} (Eh) $<S^2>_{HS}$	E_{BS} (Eh) $<S^2>_{BS}$	ΔE_{S-T} (kcal/mol)	y_p
a′	-1614.510970 *2.04*	-1614.519265 *1.39*	-10.41	0.92
b′	-1844.313856 *2.02*	-1844.358451 *0.00*	-55.96	0.34
c′	-2149.186831 *2.04*	-2149.221772 *0.00*	-43.84	0.50
d′	-2531.407408 *2.04*	-2531.479354 *0.00*	-90.28	0.25
e′	-2761.235319 *2.07*	-2761.246960 *0.63*	-14.61	0.74

for all the modeled PAH couplers, larger the radicaloid character less is their singlet-triplet gap. Thus, making open-shell singlet as the ground state of these PAH couplers. Of all the PAH couplers, decacene (a′) is found to have maximum radicaloid character followed by e′. The radicaloid character values for these couplers when nitroxy radicals are attached (y_c) to it are tabulated in Table 2. Comparing the corresponding y_p (Table 1) with y_c (Table 2), substantial decrease in the radicaloid character of decacene is observed when nitroxide radicals are attached to it. The reduction of the radicaloid character of the poly aromatic hydrocarbon when placed as magnetic spacer is due to the *spin-spilling* from the localized spin-centers. This was identified in our previous work.[44] These computed y-values indicate that the couplers retain their open-shell characteristics (with slight reduction) and magnetic identity when placed between the two localized spin-centers.

The magnetic coupling constant values for all the diradicals (**a**-**e**) computed from BS-DFT formalism are also tabulated in Table 2. Diradical **a** i.e. with decacene spacer, gives maximum magnetic coupling ($2J$) value of all the modeled diradicals. Diradical **b** having two additional benzenoid rings in the decacene backbone, shows a drastic decrease in the magnetic coupling constant value. Diradical **c** with six additional benzenoid rings capping the central tetracene region of decacene also shows an enormous decrease in the coupling

Table 2: Computed magnetic exchange coupling ($2J$) (cm^{-1}) values and energies (Eh) with corresponding $<S^2>$ values of triplet (HS) and broken-symmetry (BS) states for all the diradicals (**a-e**) with B3LYP/def2-TZVP method. Radicaloid character of couplers when nitroxide radicals are attached to it (y_c), calculated using natural orbital occupancy of frontier orbitals obtained with UHF/def2-TZVP method.

Diradical	E_{HS} (Eh) $<S^2>_{HS}$	E_{BS} (Eh) $<S^2>_{BS}$	ΔE_{BS-T} (kcal/mol)	$2J$ (cm^{-1})	y_c
a	-2107.733867 *3.32*	-2107.721359 *1.95*	7.85	5489.68	0.73
b	-2337.569787 *2.19*	-2337.569716 *1.18*	0.04	31.24	0.31
c	-2642.432382 *2.16*	-2642.432127 *1.11*	0.16	111.96	0.46
d	-3024.688704 *2.08*	-3024.688686 *1.08*	0.01	7.94	0.24
e	-3254.456724 *2.78*	-3254.453874 *1.08*	1.78	1250.8	0.69

constant value as compared to diradical **a** but it is stronger when compared with diradical **b**. Diradical **d** has the minimum $2J$ value of all the considered diradicals. Diradical **e** with a completed [3]triangulene nanostructure on either side of decacene shows a stronger coupling as compared to diradicals **b**, **c** and **d** while this value is still less than that observed for diradical **a**.

Comparing the magnetic coupling constant value with the radicaloid nature of the coupler, we observe that the $2J$ values obtained, are in direct correspondence with the radical nature of the coupler mediating the nitroxy radicals. In other words, for a given length of coupler between magnetic centers more is the radicaloid character of the coupler more will be the magnetic exchange constant value. Diradicals **a** and **e** have PAH couplers (a′ and e′) with very high radicaloid character and thus, mediate to ferromagnetically couple the nitroxide radicals strongly. The PAH couplers in diradicals **b** and **c**, show a moderate radicaloid character with intermediate magnetic exchange coupling constant. Diradical **d** shows the minmal magnetic coupling between the nitroxide radical sites which is in line with minimum radical character of the corresponding PAH coupler.

The spin of the converged wavefunction is reflected by its $<S^2>$ value. For a pure triplet spin

state, $<S^2>_{HS}$ should be *2.00* while that for broken-symmetry state $<S^2>_{BS}$ is expected to be *1.00*. Deviation from these values would reflect spin contamination in the wavefunction. The obtained $<S^2>$ values for diradicals **b**, **c** and **d** indicate that they have nearly pure spin states with less spin contamination. However for diradicals **a** and **e**, high spin contamination in observed (Table 2). Well defined BS states are achieved for diradicals **b**-**e** in terms of proper spin-reversal at nitroxy radical sites, spatial separation in the spin centers along with decontamination as compared to diradical **a**. Diradical **e** has highly contaminated

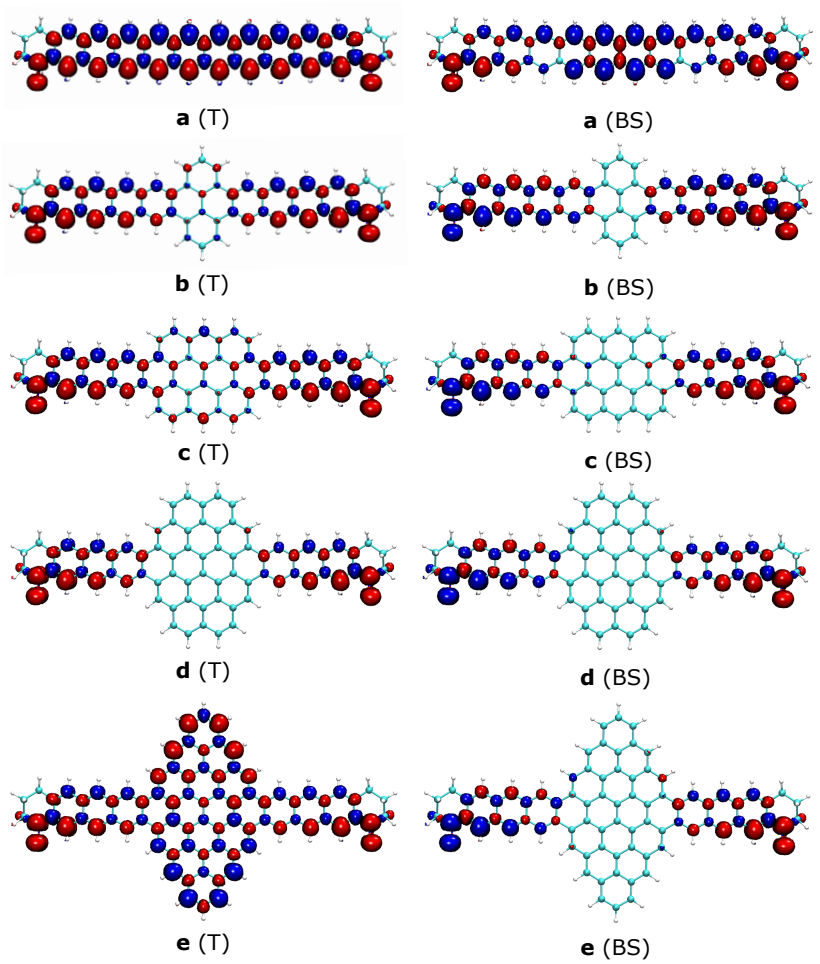

Figure 2: Spin-density plots of all the diradicals (**a**-**e**) in their triplet state (T) as well as broken-symmetry state (BS) with isosurface value 0.002 $e^-/\text{Å}^3$.

triplet state but well defined BS state. This can be understood from spin density plots of the diradicals the in their triplet and broken-symmetry states as shown in Figure 2. Spin density plots of triplet spin state for diradicals **a** and **e** show a considerable spin density in

the coupler apart from that at nitroxide centers. Whereas spin density is solely at niroxide radical centers for diradicals **b**-**d**. This explains the observed $<S^2>$ for the triplet spin state of all the diradicals. These density plots thus therefore provide us with a sneak-peak into surfacing magnetic importance of couplers themselves. The observed $<S^2>$ value for BS state of **e** is not highly contaminated as **a**, even though both the diradicals have highly contaminated triplet state. Diradicals **a** and **e** both have couplers with prominent OSS nature which is visible from these spin density plots of triplet spin state. The coupler overall is a singlet in both the cases with opposite spins delocalized in spatially different locations. Due to different spin topology leading to PAH coupler OSS nature and structural confinement, the BS states achieved in these diradicals is of different nature. A desired BS state was realized for **e** with opposite spin orientations at nitroxy radical sites as the couplers' spins are not delocalized and confined in the minimum path of magnetic communication of nitroxy radicals. While for **a**, BS state was achieved on the account of coupling of radical spins with the coupler spins giving an overall $S = 0$.

The OSS ground state properties in higher order acenes are observed with spin moments emerging in the central benzene rings with increasing acene length and getting delocalized at the zigzag edges.[57–59] This contributes to increasing radical nature of the acenes. Looking into the y values from Table 1, Löwdin spin densities at the edge carbon atoms of common decacene unit of all the studied diradicals are plotted in Figure 3. Starting from one of the nitroxy radical sites, an increase in spin density at the edge carbon atoms with a maxima at the central C atoms is observed for diradical **a** while for all other diradicals, a sharp decrease is seen with a minima at the central C atoms. The spin moment at the central C atoms decreases from 0.22 μ_B in **a** to 0.02 μ_B in **b, c, d** and **e**. For the diradicals **b, c, d** and **e**, it is conclusively visible that spin density is maximum at the nitroxy radical sites and the edge C atoms have the it's tail (Figure 2). Whereas, in diradical **a** spin-density tails originate not only from the nitroxide radical centers but as well as from this central benzene rings of the decacene coupler. Such a modulation in the coupler design of increasing π conjugation

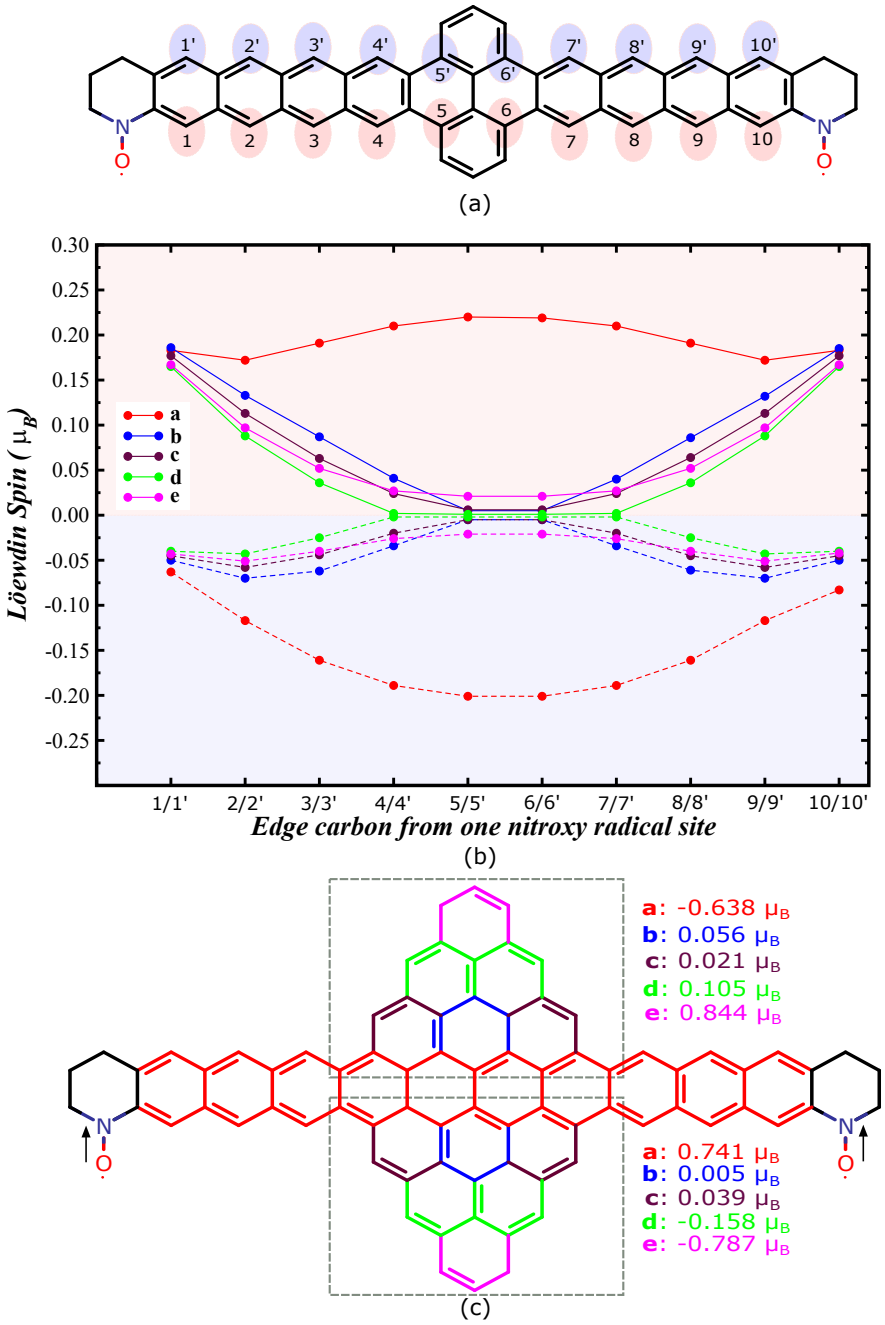

Figure 3: Löewdin spin population at different positions in the coupler. (a) Representation of carbon atom numbering on the decacene edge of diradical **b**. (b) The positive and negative values of spin moments corresponds to the decacene edge side along the nitroxy radical moieties and the opposite edge respectively. (c) Edge separated spin density in the central region of the couplers with a base of tetracene in the ground state (triplet) of diradicals. The spin density values are color coded with red, blue, maroon, green and magenta corresponding to diradicals **a**, **b**, **c**, **d** and **e**.

in the lateral direction has resulted in completely diminishing the effect of spin confinement in the decacene unit i.e. in the minimum communication path length between nitroxide radicals. Observing a striking decrease in spin-density on decacene unit of the couplers and trying to relate to the y values, spin-density in the complete central region of all the couplers was further analyzed as shown in Figure 3(c). In diradical **a** and diradical **e**, substantial spin density is observed to be delocalized in the coupler which is the principal cause for the observed y values in the these molecular systems. Whereas, in diradicals **b**, **c** and **d** no significant amount of spin density is observed to be accumulating in the coupler. The addition of benzenoid rings on base decacene for **b**, **c** and **d** has resulted in eliminating the spin aggregation in the coupler leaving only two spin centers (nitroxy sites) in these diradical systems. For **e**, spin centers happen to sprout in the coupler but at different spatial locations than in **a**. The OSS character in **e** coupler owes to the magnetic properties of [3]triangulene. With step-wise increase in the benzenoid rings in going from **a** to **e** a spin-density polarization reversal is observed in the coupler with respect to parallel spin-alignment at nitroxy radical centers (Figure 3(c)). This also explains well the spin-contamination observed in triplet state of **e**, and not for the corresponding BS state.

A deeper insight is gained into these molecular systems by looking into their molecular orbitals (MOs) (Figure 4). Ideally for organic diradical systems, the SOMOs are degenerate frontier orbitals localizing at different radical centers. Diradicals **b** and **d** having couplers with low radicaloid character adheres to this picture (refer SI). While in diradicals **a**, **c** and **e** having couplers with moderate and high radicaloid character, the orbital ordering of nitroxy SOMOs changes due to their competitive interaction with the open-shell MO's of the coupler. For these diradicals, the SOMOs stabilize and penetrate beneath the frontier open-shell MOs of the coupler. In diradicals **a** and **c**, the degeneracy of SOMOs is lifted due their asymmetric interactions with the coupler orbitals while it remains intact in diradical **e** due to symmetric orbital interactions of SOMOs with coupler magnetic orbitals. This can be realized from looking into the MOs visually. Few occupied MOs of diradical **e** are shown

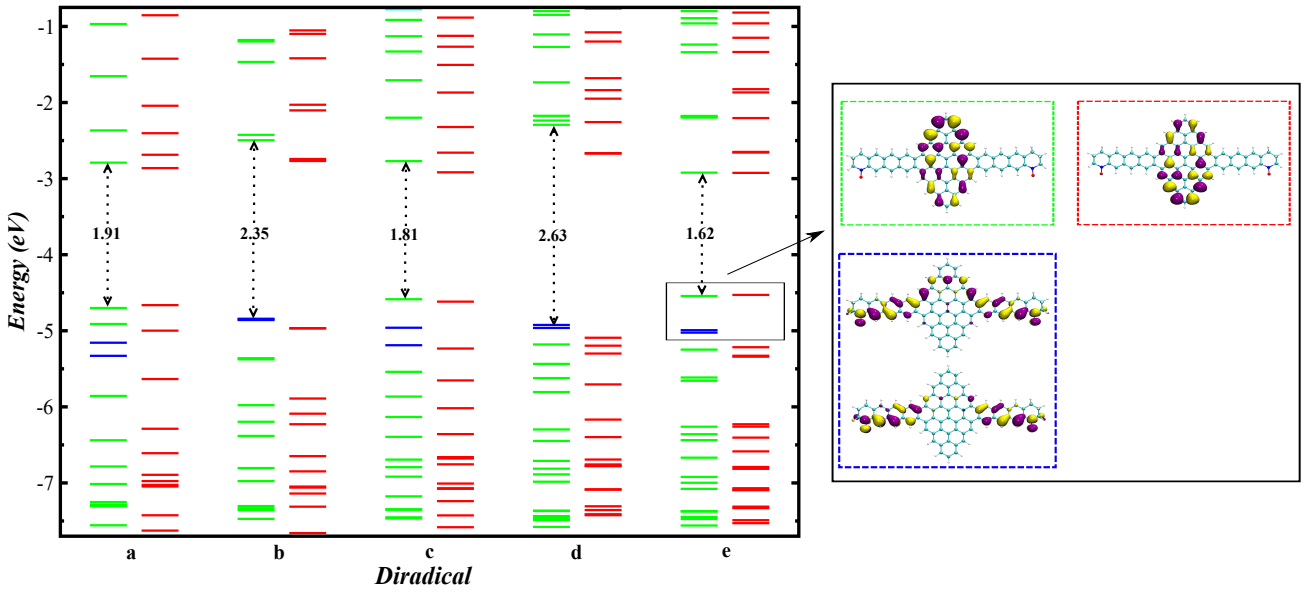

Figure 4: Molecular orbitals (MO) of spin-up (α) and spin-down (β) electrons in the triplet state of respective diradicals in the energy range of -7.5 eV to -0.8 eV. The α and β molecular orbitals are represented with green/blue and red color respectively. α MO's represented with blue correspond to the SOMOs for nitroxy radical sites. Pictorial representation of few occupied MO's for diradical **e** is also shown on the right side.

in Figure 4. Central region of the coupler in diradical **e** constitute the α and β HOMOs for this diradical. This is also the spacial region where the spin due to coupler's OSS character delocalizes (Figure 2). Therefore, these are the magnetic orbitals of the coupler, which are now the frontier orbitals for the diradical. The nitroxy SOMOs in diradical **e** are spacially well separated from the coupler magnetic orbitals. Therefore, their interaction with frontier orbitals is symmetric and hence their degeneracy is not lifted up. Diradicals **a** and **c** do not have spacially well separated nitroxy SOMOs and coupler magnetic orbitals, thereby lifting the nitroxy SOMO degeneracy in those diradicals.(MOs shown in SI) This reveals that couplers with inherent open-shell character and their magnetic orbitals play an active role in mediating the magnetic communication. Thus, radicaloid character of the coupler plays a determining role for magnetic exchange interaction through it.

Conclusions

In summary, we have realized a relationship between the OSS nature of the coupler and the magnetic exchange interaction through it. The distance between the magnetic centers i.e. nitroxy radicals is kept constant, while PAH couplers with different radicaloid character are used as spacers between them. The magnetic exchange coupling constant value is found to be more for coupler with more radicaloid character as compared to coupler with less open-shell nature. The couplers are modeled using decacene as the prototypical PAH and adding benzenoid rings in the central region on both sides of its zigzag edges. These modeled PAH couplers have reduced spin confinement in the shortest communicating path i.e. spin density at the common decacene zigzag edges drastically decreases as compared to decacene coupler. However, it is the overall radicaloid character of the coupler that dictates the strength of magnetic coupling through it. In addition to this, the MOs reveals the role of spacer magnetic orbital which compete with the SOMOs originating from radical centers for the frontier orbital ordering. Diradicals with PAH couplers having substantial radicaloid character have frontier orbitals from the coupler magnetic orbitals. This further confirms of the active role of coupler's magnetic property in determining exchange interactions through them.

Acknowledgement

Financial support from Department of Science and Technology through SERB-ECR project No. ECR/2016/000362, India-Sweden joint project No. DST/INT/SWD/VR/P-01/2016.

Supporting Information Available

Relative energies of different spin states (quintet, BS and triplet) for all diradicals and MOs for all diradicals.

References

(1) Zang, Y.; Fu, T.; Zou, Q.; Ng, F.; Li, H.; Steigerwald, M. L.; Nuckolls, C.; Venkataraman, L. Cumulene wires display increasing conductance with increasing length. *Nano Lett.* **2020**, *20*, 8415–8419.

(2) Wolf, S. A.; Awschalom, D. D.; Buhrman, R. A.; Daughton, J. M.; von Molnár, S.; Roukes, M. L.; Chtchelkanova, A. Y.; Treger, D. M. Spintronics: a spin-based electronics vision for the future. *Science* **2001**, *294*, 1488–1495.

(3) Chikamatsu, M.; Mikami, T.; Chisaka, J.; Yoshida, Y.; Azumi, R.; Yase, K.; Shimizu, A.; Kubo, T.; Morita, Y.; Nakasuji, K. Ambipolar organic field-effect transistors based on a low band gap semiconductor with balanced hole and electron mobilities. *Appl. Phys. Lett.* **2007**, *91*, 043506.

(4) Rocha, A.; Garcia-Suarez, V.; Bailey, S.; Lambert, C. J.; Ferrer, J.; Sanvito, S. Towards molecular spintronics. *Nat. Mater.* **2005**, *4*, 335–339.

(5) Bogani, L.; Wernsdorfer, W. Molecular spintronics using single-molecule magnets. *Nat. Mater.* **2008**, *7*, 179–186.

(6) Kamada, K.; Ohta, K.; Kubo, T.; Shimizu, A.; Morita, Y.; Nakasuji, K.; Kishi, R.; Ohta, S.; Furukawa, S.; Takahashi, H.; Nakano, M. Strong two-photon absorption of singlet diradical hydrocarbons. *Angew. Chem. Int. Ed.* **2007**, *46*, 3544–3546.

(7) Nakada, K.; Fujita, M.; Dresselhaus, G.; Dresselhaus, M. S. Edge state in graphene ribbons: Nanometer size effect and edge shape dependence. *Phys. Rev. B* **1996**, *54*, 17954–17961.

(8) Son, Y.; Cohen, M. L.; Louie, S. G. Half-metallic graphene nanoribbons. *Nature* **2006**, *444*, 347–349.

(9) Lombardi, F.; Lodi, A.; Ma, J.; Liu, J.; Slota, M.; Narita, A.; Myers, W. K.; Müllen, K.; Feng, X.; Bogani, L. Quantum units from the topological engineering of molecular graphenoids. *Science* **2019**, *366*, 1107–1110.

(10) Shen, J. J.; Han, Y.; Dong, S.; Phan, H.; Herng, T. S.; Xu, T.; Ding, J.; Chi, C. A stable [4,3]peri-acene diradicaloid: synthesis, structure, and electronic properties. *Angew. Chem. Int. Ed.* **2021**, *60*, 4464–4469.

(11) Morita, Y.; Suzuki, S.; Sato, K.; Takui, T. Synthetic organic spin chemistry for structurally well-defined open-shell graphene fragments. *Nat. Chem.* **2011**, *3*, 197–204.

(12) Mishra, S.; Beyer, D.; Eimre, K.; Liu, J.; Berger, R.; Gröning, O.; Pignedoli, C. A.; Müllen, K.; Fasel, R.; Feng, X.; Ruffieux, P. Synthesis and characterization of π-extended triangulene. *J. Am. Chem. Soc.* **2019**, *141*, 10621–10625.

(13) Su, J.; Fan, W.; Mutombo, P.; Peng, X.; Song, S.; Ondráček, M.; Golub, P.; Brabec, J.; Veis, L.; Telychko, M.; Jelínek, P.; Wu, J.; Lu, J. On-surface synthesis and characterization of [7]triangulene Quantum Ring. *Nano Lett.* **2021**, *21*, 861–867.

(14) Jin, H.; Li, J.; Wang, T.; Yu, Y. Photoinduced pure spin-current in triangulene-based nano-devices. *Carbon* **2018**, *137*, 1–5.

(15) Mishra, S.; Beyer, D.; Berger, R.; Liu, J.; Gröning, O.; Urgel, J. I.; Müllen, K.; Ruffieux, P.; Feng, X.; Fasel, R. Topological defect-induced magnetism in a nanographene. *J. Am. Chem. Soc.* **2020**, *142*, 1147–1152.

(16) Sun, Q.; Yao, X.; Gröning, O.; Eimre, K.; Pignedoli, C. A.; Müllen, K.; Narita, A.; Fasel, R.; Ruffieux, P. Coupled spin states in armchair graphene nanoribbons with asymmetric zigzag edge extensions. *Nano Lett.* **2020**, *20*, 6429–6436.

(17) Hu, X.; Wang, W.; Wang, D.; Zheng, Y. The electronic applications of stable diradicaloids: present and future. *J. Mater. Chem. C* **2018**, *6*, 11232–11242.

(18) Dressler, J. J.; Haley, M. M. Learning how to fine-tune diradical properties by structure refinement. *J. Phys. Org. Chem.* **2020**, *33*, e4114.

(19) Rudebusch, G. E.; Zafra, J. L.; Jorner, K.; Fukuda, K.; Marshall, J. L.; Arrechea-Marcos, I.; Espejo, G. L.; Ponce Ortiz, R.; Gómez-García, C. J.; Zakharov, L. N.; Nakano, M.; Ottosson, H.; Casado, J.; Haley, M. M. Diindeno-fusion of an anthracene as a design strategy for stable organic biradicals. *Nat. Chem.* **2016**, *8*, 753–759.

(20) Koike, H.; Chikamatsu, M.; Azumi, R.; Tsutsumi, J.; Ogawa, K.; Yamane, W.; Nishiuchi, T.; Kubo, T.; Hasegawa, T.; Kanai, K. Stable delocalized singlet biradical hydrocarbon for organic field-effect transistors. *Adv. Funct. Mater.* **2016**, *26*, 277–283.

(21) Ni, Y.; Lee, S.; Son, M.; Aratani, N.; Ishida, M.; Samanta, A.; Yamada, H.; Chang, Y.; Furuta, H.; Kim, D.; Wu, J. A diradical approach towards BODIPY-based dyes with intense near-infrared absorption around λ=1100 nm. *Angew. Chem. Int. Ed.* **2016**, *55*, 2815–2819.

(22) Yang, K.; Zhang, X.; Harbuzaru, A.; Wang, L.; Wang, Y.; Koh, C.; Guo, H.; Shi, Y.; Chen, J.; Sun, H.; Feng, K.; Ruiz Delgado, M. C.; Woo, H. Y.; Ortiz, R. P.; Guo, X. Stable organic diradicals based on fused quinoidal oligothiophene imides with high electrical conductivity. *J. Am. Chem. Soc.* **2020**, *142*, 4329–4340.

(23) Zhao, W.; Ding, J.; Zou, Y.; Di, C.; Zhu, D. Chemical doping of organic semiconductors for thermoelectric applications. *Chem. Soc. Rev.* **2020**, *49*, 7210–7228.

(24) Ullrich, T.; Pinter, P.; Messelberger, J.; Haines, P.; Kaur, R.; Hansmann, M. M.; Munz, D.; Guldi, D. M. Singlet fission in carbene-derived diradicaloids. *Angew. Chem. Int. Ed.* **2020**, *59*, 7906–7914.

(25) Ito, S.; Nakano, M. Theoretical molecular design of heteroacenes for singlet fission: tuning the diradical character by modifying π-conjugation length and aromaticity. *J. Phys. Chem. C* **2015**, *119*, 148–157.

(26) Pinheiro, M.; Das, A.; Aquino, A. J. A.; Lischka, H.; Machado, F. B. C. Interplay between aromaticity and radicaloid character in nitrogen-doped oligoacenes revealed by high-level multireference methods. *J. Phys. Chem. A* **2018**, *122*, 9464–9473.

(27) Ito, S.; Nagami, T.; Nakano, M. Diradical character-based design for singlet fission of bisanthene derivatives: aromatic-ring attachment and π-plane twisting. *J. Phys. Chem. Lett.* **2016**, *7*, 3925–3930.

(28) Pinheiro, M.; Ferrão, L. F. A.; Bettanin, F.; Aquino, A. J. A.; Machado, F. B. C.; Lischka, H. How to efficiently tune the biradicaloid nature of acenes by chemical doping with boron and nitrogen. *Phys. Chem. Chem. Phys.* **2017**, *19*, 19225–19233.

(29) Pinheiro, M.; Machado, F. B. C.; Plasser, F.; Aquino, A. J. A.; Lischka, H. A systematic analysis of excitonic properties to seek optimal singlet fission: the BN-substitution patterns in tetracene. *J. Mater. Chem. C* **2020**, *8*, 7793–7804.

(30) Milanez, B. D.; Chagas, J. C. V.; Pinheiro Jr, M.; Aquino, A. J. A.; Lischka, H.; Machado, F. B. C. Effects on the aromaticity and on the biradicaloid nature of acenes by the inclusion of a cyclobutadiene linkage. *Theor. Chem. Acc.* **2020**, *139*.

(31) Rajca, A. Organic diradicals and polyradicals: from spin coupling to magnetism? *Chem. Rev.* **2002**, *94*, 871–893.

(32) Rajca, A.; Takahashi, M.; Pink, M.; Spagnol, G.; Rajca, S. Conformationally constrained, stable, triplet ground state (S = 1) nitroxide diradicals. Antiferromagnetic chains of S = 1 diradicals. *J. Am. Chem. Soc.* **2007**, *129*, 10159–10170.

(33) Cho, D.; Ko, K. C.; Lee, J. Y. Quantum chemical approaches for controlling and evaluating intramolecular magnetic interactions in organic diradicals. *Int. J. Quantum Chem.* **2016**, *116*, 578–597.

(34) Bajaj, A.; Ali, M. E. First-principle design of blatter's diradicals with strong ferromagnetic exchange interactions. *J. Phys. Chem. C* **2019**, *123*, 15186–15194.

(35) Ali, M. E.; Datta, S. N. Polyacene spacers in intramolecular magnetic coupling. *J. Phys. Chem. A* **2006**, *110*, 13232–13237.

(36) Ali, M. E.; Datta, S. N. Broken-symmetry density functional theory investigation on bis-nitronyl nitroxide diradicals: influence of length and aromaticity of couplers. *J. Phys. Chem. A* **2006**, *110*, 2776–2784.

(37) Higashiguchi, K.; Yumoto, K.; Matsuda, K. Evaluation of the β value of the phenylene unit by probing exchange interaction between two nitroxides. *Org. Lett.* **2010**, *12*, 5284–5286.

(38) Nishizawa, S.; Hasegawa, J.; Matsuda, K. Theoretical investigation on the decaying behavior of exchange interaction in quinoid and aromatic molecular wires. *J. Phys. Chem. C* **2015**, *119*, 5117–5121.

(39) Nishizawa, S.; Hasegawa, J.; Matsuda, K. Theoretical investigation of the β value of the π-conjugated molecular wires by evaluating exchange interaction between organic radicals. *J. Phys. Chem. C* **2013**, *117*, 26280–26286.

(40) Nishizawa, S.; Hasegawa, J.; Matsuda, K. Theoretical investigation of the β value of the phenylene and phenylene ethynylene units by evaluating exchange interaction between organic radicals. *Chem. Phys. Lett.* **2013**, *555*, 187–190.

(41) Steenbock, T.; Shultz, D. A.; Kirk, M. L.; Herrmann, C. Influence of radical bridges on electron spin coupling. *J. Phys. Chem. A* **2017**, *121*, 216–225.

(42) Minkin, V. I.; Starikov, A. G.; Starikova, A. A.; Gapurenko, O. A.; Minyaev, R. M.; Boldyrev, A. I. Electronic structure and magnetic properties of the triangular

nanographenes with radical substituents: a DFT study. *Phys. Chem. Chem. Phys.* **2020**, *22*, 1288–1298.

(43) Sarbadhikary, P.; Shil, S.; Misra, A. Magnetic and transport properties of conjugated and cumulated molecules: the π-system enlightens part of the story. *Phys. Chem. Chem. Phys.* **2018**, *20*, 9364–9375.

(44) Kaur, P.; Ali, M. E. First principle investigations of long-range magnetic exchange interactions via polyacene coupler. 2020; `https://chemrxiv.org/articles/preprint/First_Principle_Investigations_of_Long-range_Magnetic_Exchange_Interactions_via_Polyacene_Coupler/12776222/2`.

(45) Liu, J.; Li, B. W.; Tan, Y. Z.; Giannakopoulos, A.; Sanchez Sanchez, C.; Beljonne, D.; Ruffieux, P.; Fasel, R.; Feng, X.; Müllen, K. Toward cove-edged low band gap graphene nanoribbons. *J.Am. Chem. Soc.* **2015**, *137*, 6097–6103.

(46) Lee, C.; Yang, W.; Parr, R. G. Development of the Colle-Salvetti correlation-energy formula into a functional of the electron density. *Phys. Rev. B* **1988**, *37*, 785–789.

(47) Hellweg, A.; Hättig, C.; Höfener, S.; Klopper, W. Optimized accurate auxiliary basis sets for RI-MP2 and RI-CC2 calculations for the atoms Rb to Rn. *Theor. Chem. Acc.* **2007**, *117*, 587–597.

(48) Weigend, F.; Ahlrichs, R. Balanced basis sets of split valence, triple zeta valence and quadruple zeta valence quality for H to Rn: Design and assessment of accuracy. *Phys. Chem. Chem. Phys.* **2005**, *7*, 3297–3305.

(49) Neese, F. Software update: the ORCA program system, version 4.0. *WIREs Comput. Mol. Sci.* **2018**, *8*, e1327.

(50) Neese, F.; Wennmohs, F.; Hansen, A.; Becker, U. Efficient, approximate and paral-

lel Hartree–Fock and hybrid DFT calculations. A 'chain-of-spheres' algorithm for the Hartree-–Fock exchange. *Chem. Phys.* **2009**, *356*, 98 – 109.

(51) Noodleman, L. Valence bond description of antiferromagnetic coupling in transition metal dimers. *J. Chem. Phys.* **1981**, *74*, 5737–5743.

(52) Valero, R.; Costa, R.; de P. R. Moreira, I.; Truhlar, D. G.; Illas, F. Performance of the M06 family of exchange-correlation functionals for predicting magnetic coupling in organic and inorganic molecules. *J. Chem. Phys.* **2008**, *128*, 114103.

(53) Ko, K. C.; Cho, D.; Lee, J. Y. Scaling approach for intramolecular magnetic coupling constants of organic diradicals. *J. Phys. Chem. A* **2013**, *117*, 3561–3568.

(54) Yamaguchi, K.; Okumura, M.; Takada, K.; Yamanaka, S. Instability in chemical bonds. II. Theoretical studies of exchange-coupled open-shell systems. *Int. J. Quantum Chem.* **1993**, *48*, 501–515.

(55) Yamanaka, S.; Okumura, M.; Nakano, M.; Yamaguchi, K. EHF theory of chemical reactions Part 4. UNO CASSCF, UNO CASPT2 and R(U)HF coupled-cluster (CC) wavefunctions. *J. Mol. Struct.* **1994**, *310*, 205 – 218.

(56) Hayashi, H.; Barker, J. E.; Cárdenas Valdivia, A.; Kishi, R.; MacMillan, S. N.; Gómez-García, C. J.; Miyauchi, H.; Nakamura, Y.; Nakano, M.; Kato, S. i.; Haley, M. M.; Casado, J. Monoradicals and Diradicals of Dibenzofluoreno[3,2-b]fluorene Isomers: Mechanisms of Electronic Delocalization. *J. Am. Chem. Soc.* **2020**, *142*, 20444–20455.

(57) Bendikov, M.; Duong, H. M.; Starkey, K.; Houk, K. N.; Carter, E. A.; Wudl, F. Oligoacenes: theoretical prediction of open-shell singlet diradical ground states. *J. Am. Chem. Soc.* **2004**, *126*, 7416–7417.

(58) Hachmann, J.; Dorando, J. J.; Avilés, M.; Chan, G. K. The radical character of the

acenes: a density matrix renormalization group study. *J. Chem. Phys.* **2007**, *127*, 134309.

(59) Trinquier, G.; David, G.; Malrieu, J. P. Qualitative views on the polyradical character of long acenes. *J. Phys. Chem. A* **2018**, *122*, 6926–6933.

Graphical TOC Entry